

# Hot Corrosion behaviour of Welded ASTM SA 210 GrA1 Boiler Tube Steels in molten salt $\text{Na}_2\text{SO}_4$ -60% $\text{V}_2\text{O}_5$ environment

**Ravindra Kumar\*, V. K. Tewari, Satya Prakash**

Metallurgical and Materials Engineering Department, Indian Institute of Technology  
Roorkee, Roorkee-247667, India

\*Corresponding author email: [ravirs\\_2002@rediffmail.com](mailto:ravirs_2002@rediffmail.com)

**Abstract:** This paper examines the hot corrosion behavior of welded steels in molten salt environment at elevated temperature. ASTM SA210 Grade A1 boiler tube steel has been selected as candidate materials, because this steel is in used in several forms in steam generator thermal power plants. Hot corrosion studies were conducted on welded GrA1 steels in molten salt environment at 900°C under cyclic conditions. The thermogravimetric technique was used to monitor kinetics of corrosion. The corrosion products formed on welded steels were characterized by scanning electron microscopy with energy dispersive of X-ray analysis (SEM/EDX), and X-ray diffraction (XRD) pattern. The TIG welded steel was found to oxidized at higher rates than that of SMAW welded steel in molten salt environment at 900°C.

**Author Keywords:** Hot corrosion, Tungsten inert gas (TIG), Shielded metal arc welding (SMAW), Molten salt, GrA1 Boiler tube steel.

## 1. Introduction:

Materials degradation at high temperatures is a serious problem in several industries such as fossil fueled power plants, gas turbines in aircraft, refineries, and petrochemical

industries, etc are examples where corrosion limits their use or reduces their life

considerably affecting the efficiency [1]. Coal fired power plants are one of the major industries suffering from severe corrosion problems resulting in the substantial losses. However, world-wide the majority of electricity is generated in coal-fired thermal plants, in which the coal is burned to boil water and the steam so produced is expanded through a turbine, which turns a generator [2]. It is basically induced by the impurities such as Na, V, S, K, and Cl, which are present in the coal or in fuel oil used for combustion in the above mentioned applications. Sometimes metals and alloys may experience accelerated oxidation when their surfaces are coated by a thin film of fused salt in an oxidizing gas. This type of attack is called hot corrosion [3]. Thus, hot corrosion may be defined as accelerated corrosion, resulting from the presence of salt contaminants such as  $\text{Na}_2\text{SO}_4$ ,  $\text{NaCl}$ , and  $\text{V}_2\text{O}_5$  that combine to form molten deposits, which damage the protective surface oxides [4]. Ferritic steels are widely used in steam generating system as boiler tube materials; these steels have good combination of weldability and resistance to corrosion at elevated temperature . Many thousands of welds were found in typical steam generating system, failure of any welds result shutdown of plant, several welding techniques are in used to weld the components. In earlier studies it has been found that HAZ from welding may severally degrade from prolonged services [5-7].

The present study has been carried out to characterized hot corrosion behavior of welded SA210 GrA1 steels in molten salt environment at  $900^\circ\text{C}$  under cyclic conditions. A SEM Back scattered image analysis of the cross-section of the oxide scale thickness has been made to measure the oxide scales formed over the welded steels. The X-ray diffraction

been used to characterize the corrosion product after hot corrosion at 900 °C.

## 2. Experimental Procedure

### 2.1 Materials and formulation of weldments

ASTM SA 210-GrA1 (GrA1) boiler tube steel (5mm diameter x 33mm thickness) is widely used in northern power plants of India. These tube steels after machining (single conventional V-groove with bevel angle 37.5°, root face of 1mm and root gape 1mm) were welded together by tungsten inert gas welding using 99% pure argon gas with filler wire ER70S-2 with 95A and 12V, and shielded metal arc welding processes using basic coated electrode E7018 with arc current 95A and 22V. The specimens, each measuring approximately 20mm×15mm×5 mm, were cut from the weldment portions. The specimens were polished with 220 grade silicon carbide paper and emery paper then wheel polished before being to corrode.

### 2.2 Molten salt (Na<sub>2</sub>SO<sub>4</sub>-60% V<sub>2</sub>O<sub>5</sub>) hot corrosion test

Hot corrosion studies were performed in a molten salt (Na<sub>2</sub>SO<sub>4</sub>-60% V<sub>2</sub>O<sub>5</sub>) for 50 cycles under cyclic conditions. Each cycle consisted of 1h heating at 900°C in a silicon carbide tube furnace followed by 20 min cooling at room temperature. The specimens were mirror polished down to 1-μm alumina wheel cloth polishing before the corrosion run. The physical dimensions of the specimen were recorded carefully with a digital vernier caliper (Mitutoyo, Japan make, resolution 0.01 mm) to evaluate their surface areas. Thereafter, the coating of uniform thickness with 3 to 5 mg/cm<sup>2</sup> of Na<sub>2</sub>SO<sub>4</sub>-60% V<sub>2</sub>O<sub>5</sub> was applied with a camel hair brush on the preheated sample (250°C). The heating of the specimen was found essential for proper adhesion of the salt layer. Subsequently, the salt

coated specimen kept in the alumina boat was weighed before exposing to hot corrosion tests in the tube furnace kept at 900°C. During hot corrosion runs, the weight of boat and specimen was measured together at the end of each cycle with the help of an electronic balance of model 06120 (Contech), with a sensitivity of 0.001 g. Visual observations were also made after the end of each cycle. During each cycle, the data taken for the sample was used to calculate the corrosion rate. The samples after corrosion were analyzed by SEM/EDX and XRD for surface analysis.

### 3. Results

#### 3.1 Visual observations

The macrographs of corroded welded specimens are shown in Fig. 1. The colour of scale during first cycle turned blackish gray for all the welded steels and up to the end of cyclic study. In SMAW welded steel the oxide protrusions, dark black shining spots were observed on the surface of weld region after first cycle. Spalling of oxide scale started during the 7<sup>th</sup> cycle. Even little cracks were found on 29<sup>th</sup> cycles, colour of the scale was blackish gray after 50<sup>th</sup> cycles. For TIG welded steel minor cracks appeared in the scale of weld regions during 5<sup>th</sup> cycles and little spallation. Oxide protrusion dark blackish grey in colour appeared from the surface of the TIG welded steel.

#### 3.2. Thermogravimetric data analysis

Weight gain per unit area expressed in mg/cm<sup>2</sup> is plotted as a function of time expressed in number of cycles for oxidised welded steels and is shown in Fig. 2. It can be inferred from the plots that the TIG welded steel showed the maximum weight gain where SMAW welded steel showed better resistance to given aggressive environment. The behavior for SMAW welded, and TIG welded steels was almost parabolic as can be inferred from the square of

weight change ( $\text{mg}^2/\text{cm}^4$ ) plotted with number of cycles in Fig. 3. The parabolic rate

constants ( $K_p$  in  $10^{-8} \text{ g}^2 \text{ cm}^{-4} \text{ s}^{-1}$ ) for these steels are 31.686 (SMAW) and 47.731 (TIG).

### 3.3 Oxide scale thicknesses measurement

The thicknesses of the oxide scale formed on the welded steels measured from the BSEI, taken along the cross-section of the mounted samples, images for all the samples are shown in Fig. 4. Micrograph shows the scale with through cracks over the HAZ region for SMAW welded steel. The average scale thickness values measured for weld region of SMAW and TIG welded steels are 1.092mm and 1.228mm respectively. Whereas average scale thickness measured for HAZ of these welded steels from backscattered images is 1.099 mm and 1.297mm respectively.

### 3.4. X-ray diffraction analysis

The X-ray diffractograms of the scale for welded steels after exposure to molten salt ( $\text{Na}_2\text{SO}_4$ -60%  $\text{V}_2\text{O}_5$ ) at 900 °C for 50 cycles are shown in Fig. 5. In the given environment all the steels have  $\text{Fe}_2\text{O}_3$  as the main constituent of scale. In addition to this  $\text{Fe}_3\text{O}_4$  peaks were observed for TIG welded steel.

### 3.5. Surface SEM/EDX analysis

The SEM micrograph and EDX analysis welded steels exposed to  $\text{Na}_2\text{SO}_4$ -60%  $\text{V}_2\text{O}_5$  environment at 900°C given in Fig. 6 indicates the formation of predominantly  $\text{Fe}_2\text{O}_3$  scale.

SEM of the top surface for weld region of SMAW weldment in GrA1 steel after hot corrosion indicates the cracking of the scale as evident from Fig. 6 (a). The top scale was consisting of  $\text{Fe}_2\text{O}_3$  and MnO (point 1) whereas inside the cracks, oxides were appeared to be mainly of  $\text{Fe}_2\text{O}_3$ , MnO and  $\text{SiO}_2$  (point 2). The top scale of HAZ region indicates the globules consists of iron oxide  $\text{Fe}_2\text{O}_3$  (99.08%) with small amount of Mn in Fig. 6 (b).

The weld region of TIG welded steel as shown in Fig. 6 (c), (d) indicated only  $\text{Fe}_2\text{O}_3$  as well

as on the HAZ. Small amount of Na was present at the spalled portion of oxide scale of HAZ.

## 4. Discussion

From weight gain data Fig. 3 it can be inferred that both weldments follows parabolic oxidation rate law so far as the kinetic of corrosion is concerned. The corrosion rate in the given environment is more of TIG welded steel as compared to SMAW welded and it was due to the formation of higher extents of cracks of oxide scale. The XRD analysis has revealed mainly the presence of  $\text{Fe}_2\text{O}_3$  in the scale of both the weldments with extra phase  $\text{Fe}_3\text{O}_4$  in case of TIG welded steel, results of cracks formation.  $\text{Fe}_2\text{O}_3$  as the main oxide in base steel has been identified also by Sidhu and Prakash [8]. In terms of scale thickness measurements, the weld region and HAZ of SMAW welded specimen shows less oxidation than that of weld and HAZ regions of TIG welded, the reason was the more internal oxidation, cracks and spallation of oxide scale during oxidation run. In case of SMAW welded steel, EDX analysis revealed the top and inner scale are richer in iron oxide with small amount of Mn of weld region of SMAW welded steel and also in HAZ inner scale, that leads to reduce corrosion rate of this weldment, whereas in case of HAZ region of TIG welded steel, small amount of sodium with main iron oxide was observed in inner scale, this may results of higher corrosion rate. The result of XRD was in accordance with the surface EDX analysis.

## 5. Conclusions

From the present studies the following points are concluded



TIG welded steel showed the more weight gain than that of SMAW welded and it was due to the formation of higher extent of cracks and spallation of oxide scale and a thicker oxide scale was found on HAZ.

The weight gain of the welded steels follows the parabolic rate law in molten salt  $\text{Na}_2\text{SO}_4 + 60\% \text{V}_2\text{O}_5$  at 900 °C. The susceptibility to hot corrosion of welded Gr A1 steel specimens has been found to be as in the following order SMAW > TIG.

## References

1. A. S. Khanna, "Introduction to high temperature oxidation and corrosion", ASM International, 2002.
2. J. Stringer, Proceedings International conference on corrosion 'CONCORN'99, Mumbai, India, December 3-6, 1997, pp 13-23.
3. R. A. Rapp, Mater. Sci. Eng., 1987, 87, 319.
4. N. Eliaz, G. Shemesh, R.M. Latenision, Eng. Fail. Anal., 2002, 9, 31.
5. H. B. Cary, Modern welding technology. Prentice Hall, Inc, Englewood cliffs, New Jersey 1979.
6. D.J. Young, High temperature oxidation and corrosion of metals, Elsevier publisher, 2008.
7. A.K. Khare, Ferritic steels for High Temperature Applications," ASM Metal Park, OH, Conf., Warren, PA 1981.
8. B.S. Sidhu, S. Prakash, Surf. Coat. Technol., 2003, 166, 89.

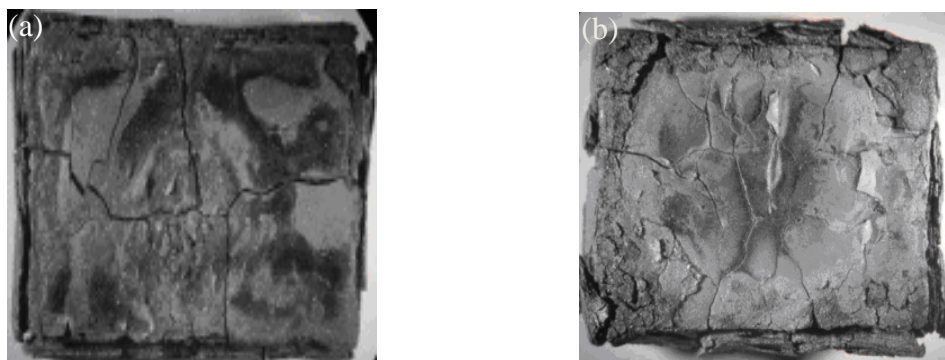


Fig. 1 Macrographs of welded GrA1 boiler tube steels subjected to cyclic hot corrosion in  $\text{Na}_2\text{SO}_4$ -60%  $\text{V}_2\text{O}_5$  at 900°C for 50 cycles (a) SMAW (b) TIG.



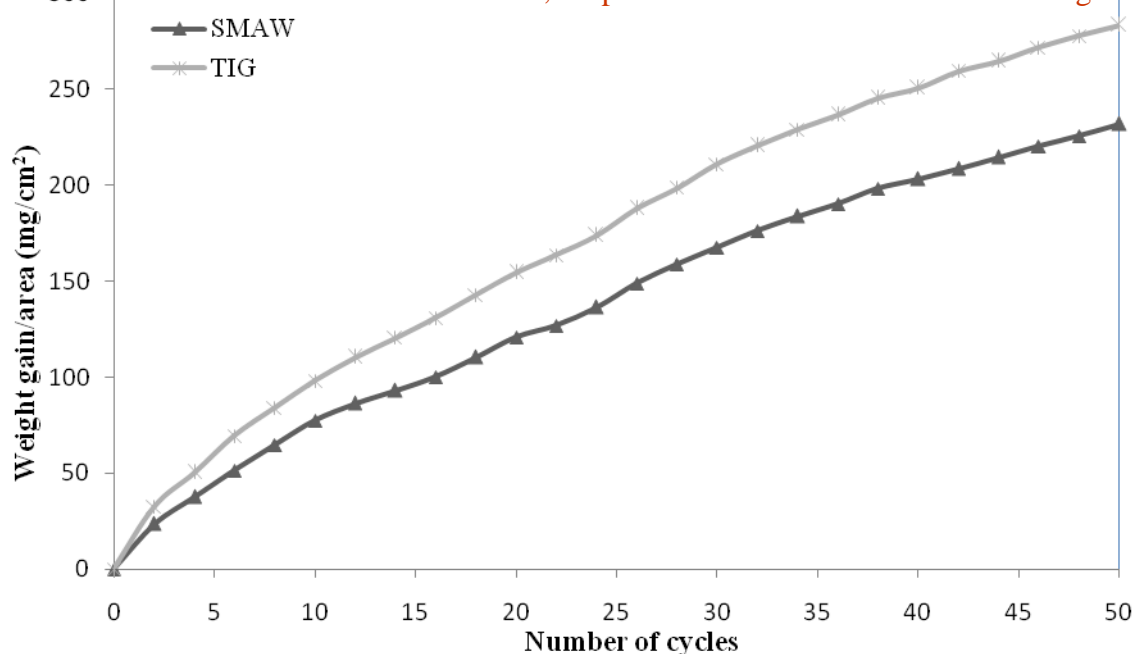


Fig. 2 Weight gain plot for welded GrA1 steels exposed to cyclic hot corrosion in  $\text{Na}_2\text{SO}_4$ -60%  $\text{V}_2\text{O}_5$  at 900°C for 50 cycles.

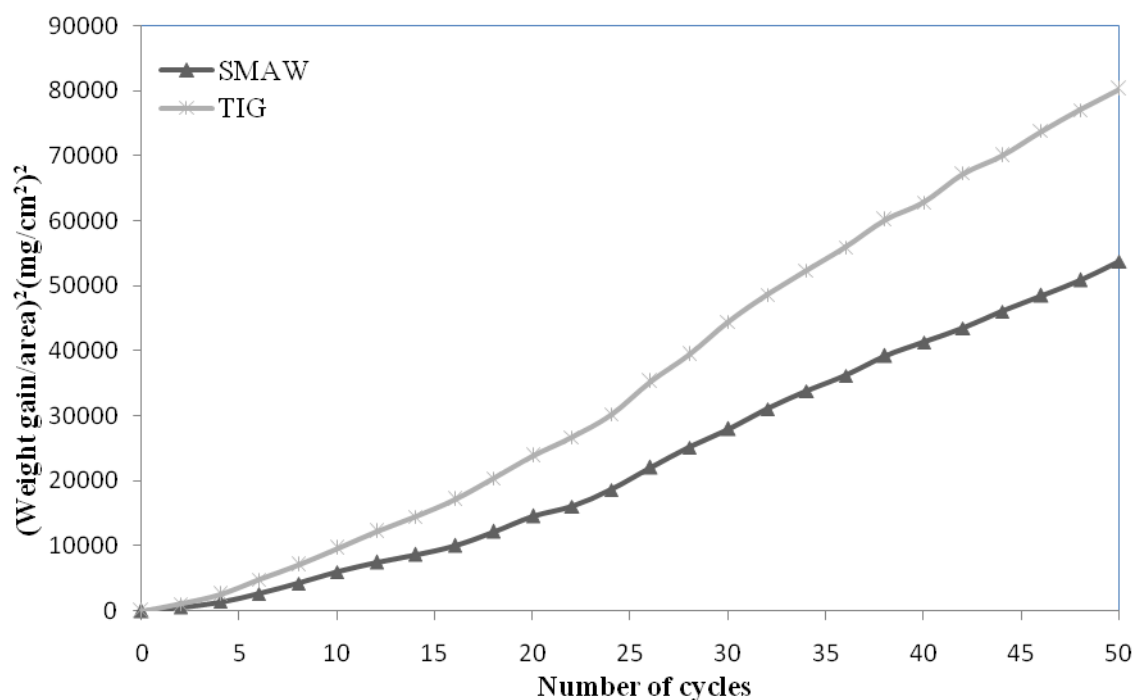


Fig. 3 Weight gain square ( $\text{mg}^2/\text{cm}^4$ ) plot for welded GrA1 steels exposed to cyclic hot corrosion in  $\text{Na}_2\text{SO}_4$ -60%  $\text{V}_2\text{O}_5$  at 900°C for 50 cycles

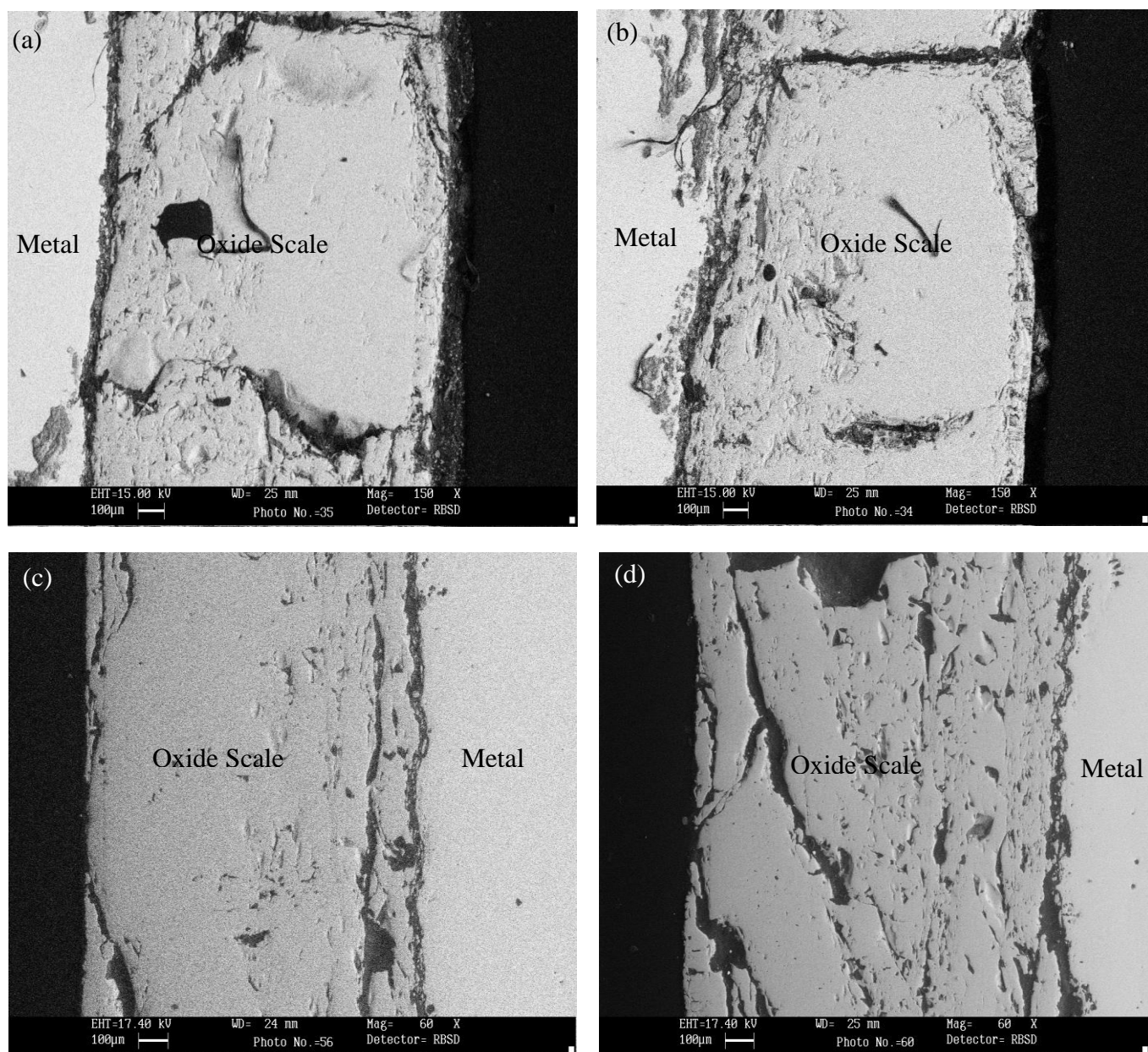


Fig. 4 SEM back scattered image of the cross section of welded steels exposed to  $\text{Na}_2\text{SO}_4$  -60%  $\text{V}_2\text{O}_5$  at  $900^\circ\text{C}$  for 50 cycles. (a) weld metal (SMAW), 150X. (b) HAZ (SMAW), 150X (c) weld metal (TIG), 60X (d) HAZ (TIG), 60X

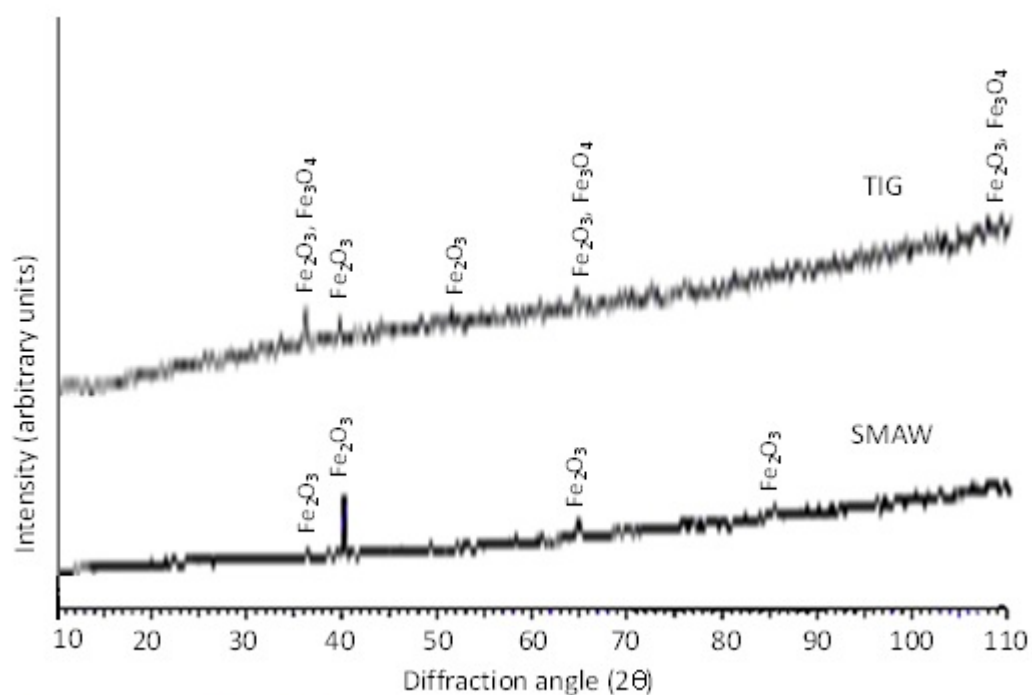


Fig.5 X-ray diffraction profiles for welded GrA1 steels exposed to cyclic hot corrosion in  $\text{Na}_2\text{SO}_4$ -60%  $\text{V}_2\text{O}_5$  at 900°C for 50 cycles



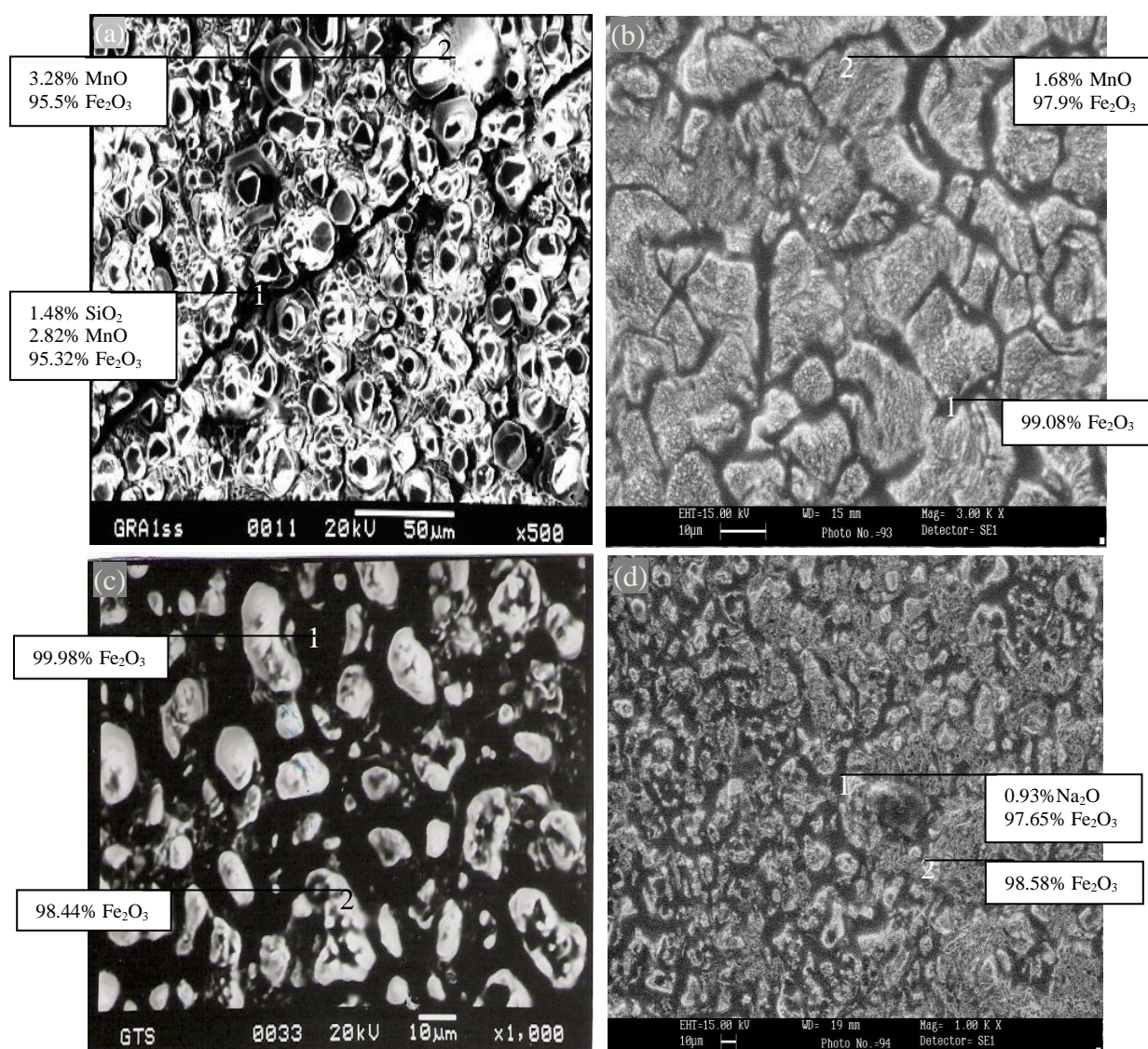


Fig. 6 Surface morphology and EDAX analysis for welded GrA1steels exposed to Na<sub>2</sub>SO<sub>4</sub> + 60% V<sub>2</sub>O<sub>5</sub> at 900°C for 50 cycles (a) Weld Metal (SMAW), 500X (b) HAZ (SMAW), 3000X (c) Weld metal (TIG), 1000X (d) HAZ, 1000X.